

# Improved Forecasts of the Diurnal Cycle in the Tropics Using Multiple Global Models. Part I: Precipitation

T. N. KRISHNAMURTI

*Department of Meteorology, The Florida State University, Tallahassee, Florida*

C. GNANASEELAN

*Department of Meteorology, The Florida State University, Tallahassee, Florida, and Indian Institute of Tropical Meteorology, Pune, India*

A. K. MISHRA AND A. CHAKRABORTY

*Department of Meteorology, The Florida State University, Tallahassee, Florida*

(Manuscript received 19 June 2007, in final form 10 December 2007)

## ABSTRACT

The Tropical Rainfall Measuring Mission (TRMM) satellite supplemented with the Defense Meteorological Satellites Program (DMSP) microwave dataset provides accurate rain-rate estimates. Furthermore, infrared radiances from the geostationary satellites provide the possibility for mapping the diurnal change of tropical rainfall. Modeling of the phase and amplitude of the tropical rainfall is the theme of this paper. The present study utilizes a suite of global multimodels that are identical in all respects except for their cumulus parameterization algorithms. Six different cumulus parameterizations are tested in this study. These include the Florida State University (FSU) Modified Kuo Scheme (KUO), Goddard Space Flight Center (GSFC) Relaxed Arakawa–Schubert Scheme (RAS1), Naval Research Laboratory–Navy Operational Global Atmospheric Prediction System (NRL–NOGAPS) Relaxed Arakawa–Schubert Scheme (RAS2), NCEP Simplified Arakawa–Schubert Scheme (SAS), NCAR Zhang–McFarlane Scheme (ZM), and NRL–NOGAPS Emanuel Scheme (ECS). The authors carried out nearly 600 experiments with these six versions of the T170 Florida State University global spectral model. These are 5-day NWP experiments where the diurnal change datasets were archived at 3-hourly intervals. This study includes the estimation of skills of the phase and amplitudes of the diurnal rain using these member models, their ensemble mean, a multimodel superensemble, and those from a single unified model. Test results are presented for the global tropics and for some specific regions where the member models show difficulty in predicting the diurnal change of rainfall. The main contribution is the considerable improvement of the modeling of diurnal rain by deploying a multimodel superensemble and by constructing a single unified model. The authors also present a comparison of these findings on the modeling of diurnal rain from another suite of multimodels that utilized different versions of cloud radiation algorithms (instead of different cumulus parameterization schemes) toward defining the suite of multimodels. The principal result is that the superensemble does provide a future forecast for the total daily rain and for the diurnal change of rain through day 5 that is superior to forecasts provided by the best model. The training of the superensemble with good observed estimates of rain, such as those from TRMM, is necessary for such forecasts.

## 1. Introduction

This is a sequel to a number of recent studies on multimodel forecast performances where different physical parameterizations are carried out by different

member models. Krishnamurti and Sanjay (2003) utilized six different cumulus parameterization schemes in the Florida State University (FSU) global spectral model (FSUGSM). About 100 short-range numerical prediction experiments were performed with each of the six models. In all of these experiments, the model physics (except the cumulus parameterization) and the initial state for each set of the six forecasts were kept the same. The model validations were carried out with

---

*Corresponding author address:* T. N. Krishnamurti, Department of Meteorology, The Florida State University, Tallahassee, FL 32306.

E-mail: [tnk@io.met.fsu.edu](mailto:tnk@io.met.fsu.edu)

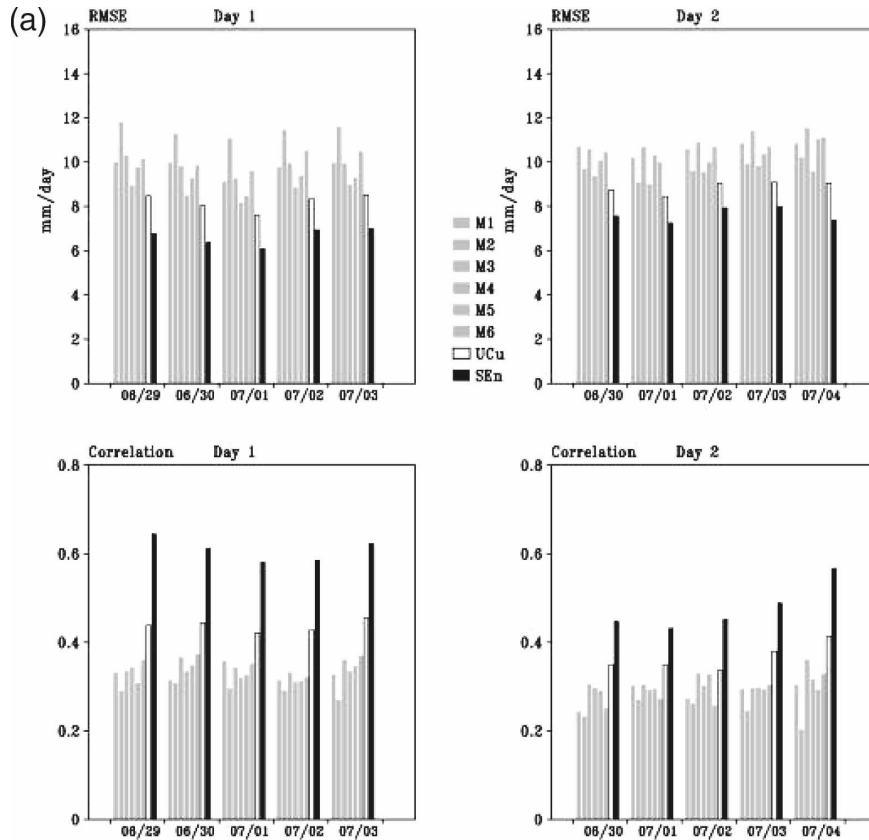


FIG. 1. The results of precipitation forecast skills for days 1 and 2 of the forecasts over the (a) global tropics and (b) North American and (c) Asian regions: forecasts dates are indicated at the bottom of each panel. The left six vertical bars in each panel show the performance of the member models, the barb with no shading pertains to the unified model, and the black barb represents the multimodel superensemble. Units:  $\text{mm day}^{-1}$ .

the best observed precipitation estimates that were obtained from a mix of satellite and rain gauge observations. The first part of this study established that a version of the Arakawa–Schubert cumulus parameterization schemes provided slightly superior precipitation for days 1 and 2 of the forecasts. However, a forecast from the ensemble mean shows higher skills for these rainfall forecasts compared to the best model. At this stage the precipitation based on the FSU superensemble (Krishnamurti et al. 2003) was constructed for these multimodels. It was noted that the superensemble carried the highest skill compared to the ensemble mean and the individual member models. The superensemble provides weights during its training phase. Those weights for the different member models can be positive or negative or even fractional (Krishnamurti and Sanjay 2003). It is possible to use these weights and construct a single forecast model that uses a weighted average (based on these weights) for a unified model. Such a unified model was shown to carry a skill higher than those of the member models and their ensemble

mean but lower than a multimodel superensemble. These results are shown in Figs. 1 and 2 for days 1 and 2 of rainfall forecasts over the global tropics, North America, and the Asian monsoon domain.

In a related study, Chakraborty et al. (2007) examined four versions of the FSU model where the cloud radiative transfer algorithms were different for each version. These versions include the cloud schemes based on Slingo et al. (1987) and Pleim and Xiu (1995). This study was aimed at comparing the results of short-range predictions from the use of ensemble mean, a unified model, and the multimodel superensemble. In this study the prediction of the diurnal changes for the phase and amplitude (fractional coverage) of low, middle, and high clouds was vastly improved for the construction of a multimodel superensemble compared to predictions of the member models. Special focus has been given to the regions of the eastern Tibetan Plateau, the eastern foothills of the Himalayas, and central Brazil where the member models produced large errors. The ensemble mean provided a slight improve-

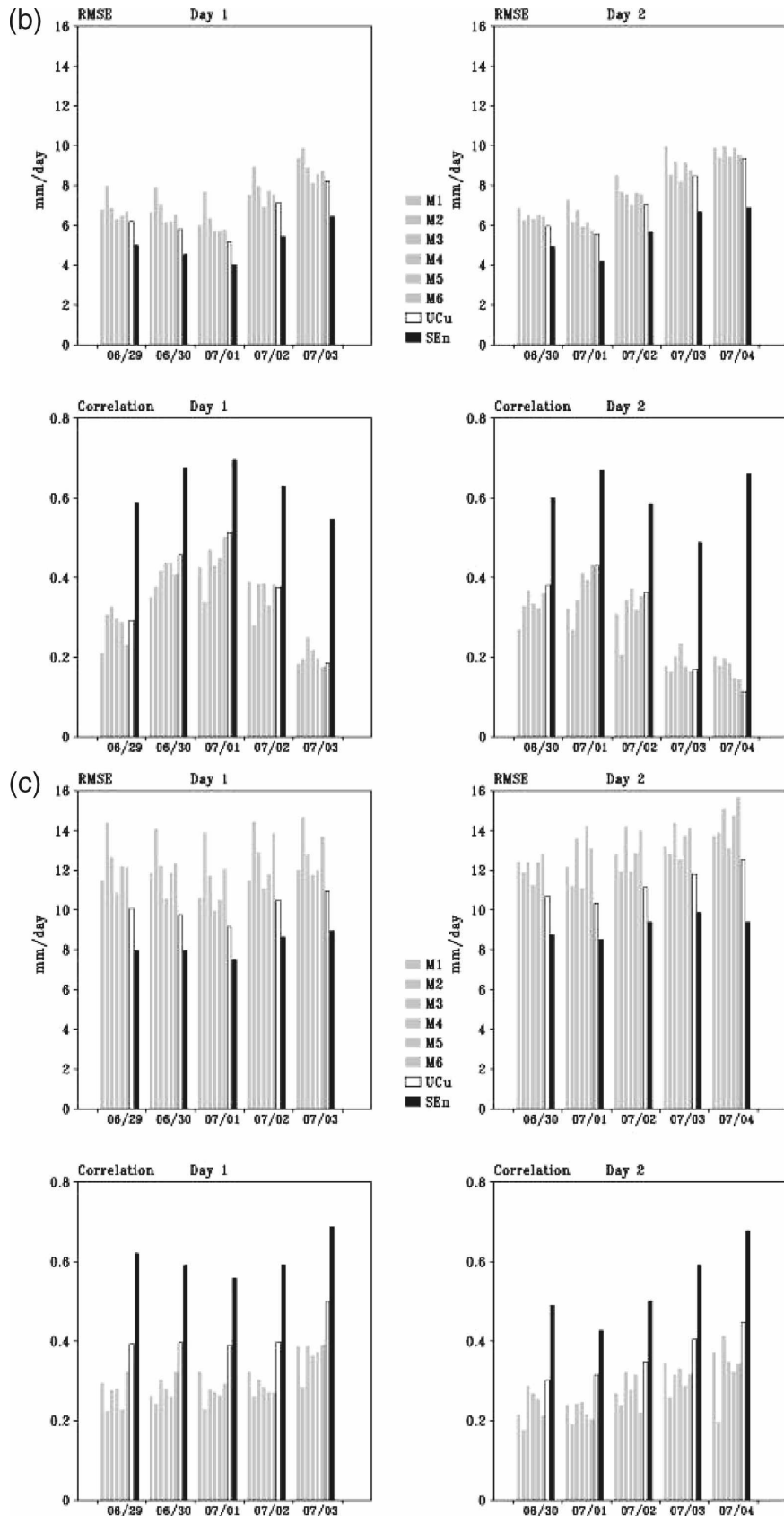


FIG. 1. (Continued)

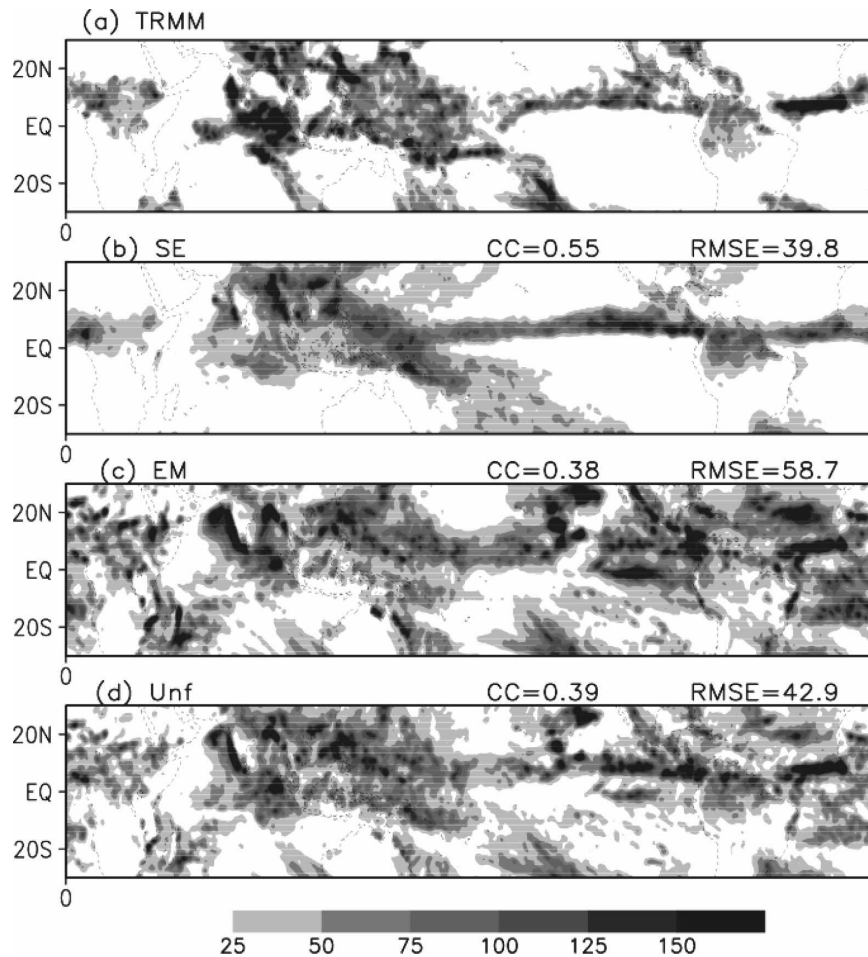


FIG. 2. A sample of the (a) TRMM-observed total rainfall estimates and those produced from a model for day 2 of the forecasts using the (b) superensemble, (c) ensemble mean, and (d) unified model. Units:  $\text{mm day}^{-1}$ .

ment in the forecast of the diurnal change over that of the member models. The unified model carried a higher skill compared to the individual models and their ensemble mean, whereas the multimodel superensemble showed a close match to the observed phase and amplitude over these three regions. This reduction of error has to do with the similar sustained systematic errors by the member models that are easily reduced by the superensemble. Part II of this paper (Chakraborty and Krishnamurti 2008) used these four cloud parameterization schemes to study the continental-scale diurnal mode for the Asian monsoon region. Another such study on the use of diverse physical parameterization within a suite of multimodels was reported in Krishnamurti et al. (2008). Here several planetary boundary layer algorithms constituted the difference among the member models of a multimodel suite. The goal of this study was to examine the possible improvements in the planetary boundary layer fluxes of latent heat that can

be achieved from our approach. This study requires an observational benchmark for the latent heat fluxes. Those were obtained from the vertical integrals of the apparent moisture sink relation of Yanai (1963) where the computation of the PBL fluxes were obtained from the reanalysis datasets and using the observed rainfall estimates from the Tropical Rainfall Measuring Mission (TRMM). Basically the results of this study again confirmed the same hierarchy of results; that is, the predicted flux of latent heat improved as we moved sequentially from the member models, the ensemble mean, and the unified model and to the multimodel superensemble.

## 2. Various cumulus parameterization schemes used in the present study

### a. FSU Modified Kuo Scheme

The operational version of the Florida State University global spectral model is equipped with the Modi-

fied Kuo Scheme (KUO) (Krishnamurti et al. 1980; Krishnamurti and Bedi 1988), which includes vertical advection of moisture and differences in temperature and specific humidity between a local moist adiabat and the environmental sounding. For the definition of clouds, moisture supply is given by vertical advection of moisture, whereas the difference of temperature and specific humidity define the heating and moistening of a unit vertical column. The Modified Kuo Scheme furthermore invokes a mesoscale moisture convergence and a moistening parameter based on conservation laws for moisture and heat that, in turn, define the evolving amplitudes for the column heating and moistening. A closure is required for determining these amplitudes, which involves additional large-scale features such as the vertically averaged vertical velocity and the lower-tropospheric cyclonic vorticity. This scheme has been tested in numerous studies on tropical weather disturbances by the FSU group.

#### *b. GSFC Relaxed Arakawa–Schubert Scheme*

The Goddard Space Flight Center (GSFC) Relaxed Arakawa–Schubert Scheme (RAS1) is a simplified form of the Arakawa and Schubert (1974) cumulus parameterization (AS), which was introduced by Moorthi and Suarez (1992). The complex cloud model in AS is simplified by assuming that the normalized cloud updraft mass flux is a linear function of height, and the effects of cloud condensate loading and moisture content in the buoyancy calculations are ignored. Quasi equilibrium is achieved through relaxation of the sounding toward the equilibrium state in a prescribed time instead of simultaneously letting all cloud ensembles adjust the environment to a state of equilibrium. This original implementation of RAS1 is used in the model version using the GSFC cumulus code. This version is known to have excessive drying owing to the lack of downdraft effects and because of not including the effects of evaporation of falling rain in the environment, which was also a problem with the original AS scheme. In spite of these problems we have used this original RAS1 version to bring out the diversity in model forecasts when such observed features are not present.

#### *c. NRL–NOGAPS Relaxed Arakawa–Schubert Scheme*

The Naval Research Laboratory–Navy Operational Global Atmospheric Prediction System (NRL–NOGAPS) Relaxed Arakawa–Schubert Scheme (RAS2) uses a variant of the original AS scheme based on a discrete form of the parameterization developed by Lord and Arakawa (1980) and Lord et al. (1982). The closure is simplified by allowing the environment

to be modified through relaxation similar to the RAS scheme by Moorthi and Suarez (1992). In this formulation, the ensemble cloud model is generalized to include the effects of a simple cloud-scale moist downdraft. It also includes the low-level moistening effects due to the evaporation of convective precipitation. The moist static energy is conserved during both of these moist processes.

#### *d. NCEP Simplified Arakawa–Schubert Scheme*

In the National Centers for Environmental Prediction (NCEP) Simplified Arakawa–Schubert Scheme (SAS), penetrative convection is simulated following Pan and Wu (1995), which is based on AS as simplified by Grell (1993) and with a saturated downdraft. The cloud ensemble is reduced to only one cloud type with detrainment only from its top. Similar to the original AS scheme, it includes the effects of moisture detrainment from convective clouds, warming from environmental subsidence, and convective stabilization in balance with the large-scale destabilization rate. Differing from the general AS formulation, which requires the presence of large-scale atmospheric destabilization with time, SAS uses the rate of change in stability as a major factor to determine a convection trigger. It differs from the Grell scheme in the triggering details and the link to large-scale variables. While AS schemes, including Grell, respond to changes in CAPE, the SAS responds, instead, to differences between model CAPE and a climatological CAPE (from tropical oceans) that varies with cloud height. Over land the scheme allows the atmosphere to completely eliminate CAPE and buoyancy in the presence of large-scale upward vertical motion at the cloud base.

#### *e. NCAR Zhang–McFarlane Scheme*

The National Center for Atmospheric Research (NCAR) Zhang–McFarlane Scheme (ZM) is a simplified cumulus parameterization scheme developed for climate modeling and reported in Zhang and McFarlane (1995). This scheme is based on a plume ensemble concept somewhat similar to the original proposition of AS and addresses penetrative deep convection. The scheme, first tested on a column model, attains equilibrium where large-scale humidity in the tropics in the presence of convection is less than the saturation limit. It includes an ensemble of entraining updrafts with an evaporatively driven ensemble of convective-scale downdrafts. Here the scheme is simplified to address the issues of quasi equilibrium by stating that the same initial mass flux characterizes the cloud-base mass flux for updrafts and cloud-top mass flux for downdrafts. Furthermore, it is assumed that the fractional entrain-

ment rates are limited to certain values dictated by large-scale thermodynamical structure. In this formulation quasi equilibrium is accomplished when the production of convective available energy balances the consumption of this quantity by moist convection. Convective available energy is generated by the combined actions of surface fluxes of heat, moisture, radiative cooling, and large-scale ascent. The rest of the formulation is quite similar to that of the simplified AS scheme.

#### f. *NRL–NOGAPS Emanuel Scheme*

The NRL–NOGAPS Emanuel Scheme (ECS) is described in two papers, Emanuel (1991) and Emanuel and Zivkovic-Rothman (1999). Here deep cumulus convection is designed to penetrate the level of neutral buoyancy of the parcel originating as an undiluted sub-cloud-layer air. Entrained air is what mostly constitutes the mass of these convective clouds. This scheme permits strong saturated downdrafts even in the absence of rain. Stabilization of the boundary layer is accomplished by evaporation of falling rain initiated by the unsaturated downdrafts. An important ingredient of this scheme is the “buoyancy sorting,” a notion introduced by Raymond and Blyth (1986), which assumes that a spectrum of cloud air mixes with different mixing fractions by ascending or descending to the level of vanishing buoyancy. Mixing in clouds is highly intermittent and inhomogeneous in this scheme. Two precipitation formation processes are central in this scheme, that is, the Bergeron–Findeisen and a stochastic coalescence mechanism. This scheme uses a mass flux parameterization where the flux transport is across various sorted levels; this is accomplished by a predictive equation for the mass flux. The roots of convection are assumed to arise from a level where the maximum value of moist static energy is found below the level of an equivalent potential temperature ( $\theta_e$ ) minimum. This permits several possible vertical levels where initiation of convection can occur. Precipitation is generated from prescribed cloud water thresholds for each sample of cloud air.

#### g. *Experimental details*

The above six cumulus convection parameterization schemes are used to construct multimodel ensemble forecasts with the T170 FSUGSM. Five-day-long forecasts were carried out with all six versions of the model starting at 1200 UTC 1 May 2001 and continuing until 1200 UTC 31 August 2001. Initial conditions were extracted from the 40-yr European Centre for Medium-Range Weather Forecasts (ECMWF) Re-Analysis (ERA-40). Sea surface temperature (SST) boundary

conditions were obtained from the Reynolds and Smith (1994) weekly datasets and interpolated linearly to the model run time. Model outputs were stored at 3-h intervals for understanding the diurnal cycle. Starting at 1500 UTC of the day of the initial condition to 1200 UTC the next day, all eight (3 h) forecast time points together are termed as day 1 forecasts. Day 2 forecasts follow day 1 forecasts and similarly for other forecast lead times up to day 5.

### 3. **The multimodel superensemble and a single unified model**

Predictions from an ensemble of slightly different initial conditions and/or various versions of models using a single base model are often carried out by the weather services. An ensemble mean is defined as the average of all models involved in the ensemble suite. Another type of ensemble mean is the bias-removed ensemble mean, where the bias of each model is removed prior to the execution of an ensemble average. In both of these cases all models are given an equal weight of  $1/N$ , where  $N$  denotes the total number of models. The superensemble approach is a recent contribution to the general area of weather and climate forecasting developed at FSU; this has been discussed in a series of publications (Krishnamurti et al. 1999, 2000a,b, 2001). This technique entails the partition of a time line into two parts. One part is a “training” phase, where forecasts by a set of member models are compared to the observed or the analysis fields with the objective of developing statistics (i.e., weights  $a_i$ ) on the least squares fit of the forecasts to the observations. The second part is the forecast phase, where estimates for  $a_i$  from the training phase are used to create the superensemble. The performance of the individual models is obtained in the training phase using multiple linear regressions against observed (analysis) fields. The outcome of this regression is the weights assigned to the individual models in the ensemble, which are then passed on to the forecast phase to construct the superensemble forecasts. The temporal model anomalies of the variables are regressed against the observed anomalies when formulating the superensemble forecasts, and the weights are multiplied to the corresponding model anomalies. The constructed forecast,  $S$ , is

$$S = \bar{O} + \sum_{i=1}^N a_i(F_i - \bar{F}_i), \quad (1)$$

where  $\bar{O}$  is the observed climatology over the training period,  $a_i$  is the weight for the  $i$ th member in the ensemble, and  $F_i$  and  $\bar{F}_i$  are the  $i$ th model's forecasts and the forecast mean (over the training period);  $N$  is the

number of member models. The weights  $a_i$  are obtained by minimizing the error term  $G$ , where  $G$  is expressed as

$$G = \sum_{t=1}^{N_{\text{train}}} (S'_t - O'_t)^2. \quad (2)$$

Here  $N_{\text{train}}$  is the number of time samples in the training phase, and  $S'_t$  and  $O'_t$  are the respective superensemble and observed field anomalies at training time  $t$ .

This exercise is performed at all model grid points. A fit performed for all model variables at all model grid points at all vertical levels typically yields close to  $10^7$  regression weights. These spreads of weights are fractional, positive, or negative. The large number arises from the number of transform grid points, vertical levels, basic variables, and the number of models. Over many such locations we have noted diverse performance characteristics of the member models. These arise from differences in horizontal and vertical discretization, treatment of physics, handling of the inhomogeneity of land surface, orography, water bodies, surface physics, and boundary conditions. All such peculiarities tend to leave their signature in the error distributions and hence on these weights. These may be thought of as a collective bias-correction procedure. The second part of the time line is composed of model predictions. The superensemble approach combines each of these forecasts according to the weights determined during the training phase using the formulation. The prediction  $S$  is referred to as the “superensemble” forecast. This forecast should be contrasted with the more standard anomaly forecasts known as the bias-removed ensemble mean or ensemble mean forecast:

$$E = \bar{O} + \frac{1}{N} \sum_{i=1}^N (F_i - \bar{F}_i). \quad (3)$$

Skill of the multimodel superensemble method significantly depends on the error covariance matrix since the weights of each model are computed from a designed covariance matrix. The classical method for the construction of the superensemble utilizes a least square minimization principle within a multiple regression of model output against observed “analysis” estimates. This entails a matrix inversion that is solved by the Gauss–Jordan elimination technique. That matrix can be ill conditioned and singular depending on the interrelationships of the member models of the superensemble. We have recently designed a singular value decomposition (SVD) method (Wilks 1995) for the multimodel superensemble that overcomes this problem and removes the ill conditioning of the covariance matrix entirely (Yun et al. 2003). Tests of this method have shown great skill in weather and seasonal climate

forecasts compared to the Gauss–Jordan elimination method.

#### *A unified model*

This is a single model that carries a weighted sum of all six cumulus parameterization schemes (Krishnamurti and Sanjay 2003). The weight varies in the three dimensions as well as for the day of forecasts. These weights are provided by the multimodel superensemble forecasts of convective rain. This single model’s cumulus parameterization is physically based since it carries the essence of most of the current schemes. In that study we had examined the forecast skill of total daily rain from this single unified model compared to member models that carry a single cumulus parameterization scheme. Based on nearly 100 forecast experiments it was concluded that the unified model performed better, in terms of conventional skill scores, compared to any of the original models. Thus, it became possible to design a single model that was superior to the member models. In the present paper we are interested in looking at the forecasts of phase and amplitude of the diurnal change of rainfall over the tropics. The question asked here is that, if a unified cumulus parameterization scheme is used that improves the total rain, would that unified model improve the diurnal rain compared to the member models. The member models generally carry rather large phase and amplitude errors for the diurnal change. In short, the ensemble mean of each parameter is simply the mean of all member models. The superensemble gives rather more weight to a model that performs better. The unified model, in fact, acts as a single model that inherently combines different physically based parameterization schemes using the weights derived by the superensemble. Since this scheme is flexible in terms of the number of models in the ensemble, any number of input member models can, in principle, be used to construct the unified model.

## **4. Predicting diurnal and total rain**

### *a. Total rainfall*

Here we show the observed TRMM (3B42)–based rainfall estimate in Fig. 2a. The day 2 forecast based on the multimodel superensemble (SE) is displayed in Fig. 2b. The forecasts based on the ensemble mean are shown in Fig. 2c. It should be noted that the ensemble mean represents a skill somewhat higher than the best model; for that reason we have not displayed the results from the individual member models. Figure 2d provides the result from the unified model. A quick look at these rainfall distributions shows clearly an excessive spread

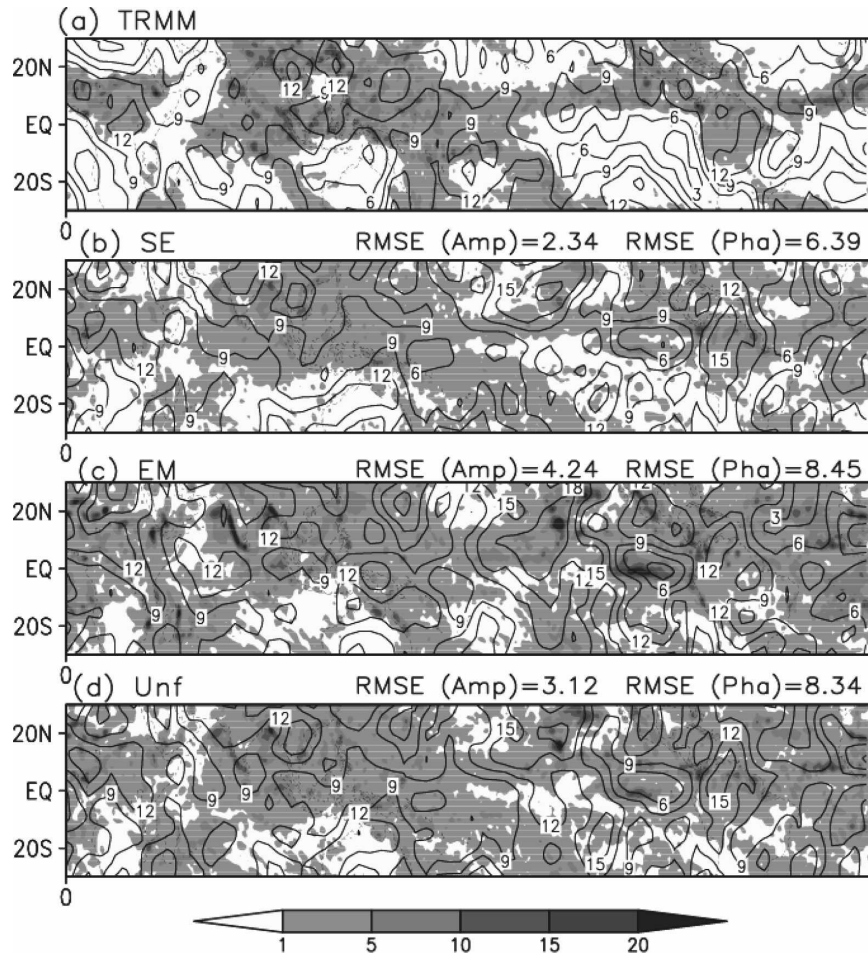


FIG. 3. Amplitude and phase of the diurnal (a) TRMM-observed rainfall estimates and those produced for day 2 of the forecasts using the (b) superensemble, (c) ensemble mean, and (d) unified model. Phase angles are shown as isopleths, i.e., local time of day (i.e., 3, 6, 9, 12, 15, or 18 h); amplitude is shaded. Units:  $\text{mm day}^{-1}$ .

of rainfall over most of the tropics between the equator and  $20^{\circ}\text{N}$  for the ensemble mean and the unified model. The agreement of the superensemble-based forecasts and observed TRMM estimates seems to be closest among the forecasts displayed here. The skills based on root-mean-square (rms) errors of day 2 rainfall forecasts were 39.8, 58.7, and  $42.9 \text{ mm day}^{-1}$  for the multimodel superensemble, the ensemble mean, and the unified model, respectively. The corresponding values for the pattern correlation (which is the spatial correlation designed to detect the similarities in the patterns of the field) of rain were 0.55, 0.38, and 0.39, respectively. The single model (the unified model) can be designed to carry a skill slightly higher than the ensemble mean of the member models. Similar skills were noted for days 1 through 5 of rainfall forecasts for the entire tropics. The performance of the superensemble

and unified models is comparable to Krishnamurti and Sanjay (2003).

#### b. Predicting the geographical distribution of the amplitude and phase of diurnal rainfall

The geographical distribution of the amplitude and phase of the diurnal mode for TRMM datasets and from the superensemble (SE), the ensemble means (EM), and the unified model (Unf) for day 2 of the forecasts is illustrated in Fig. 3. In this figure, the phase angles are shown by isopleths, that is, local time of day (i.e., 3, 6, 9, 12, 15, or 18 h) as indicated by labels on the isopleths. A Fourier transform on the time series of 3-hourly forecasts was made on every day of the series to extract the diurnal cycle. The diurnal cycle is defined here as the first harmonic of the transformed series. Next, an hour-by-hour average of the first harmonic of

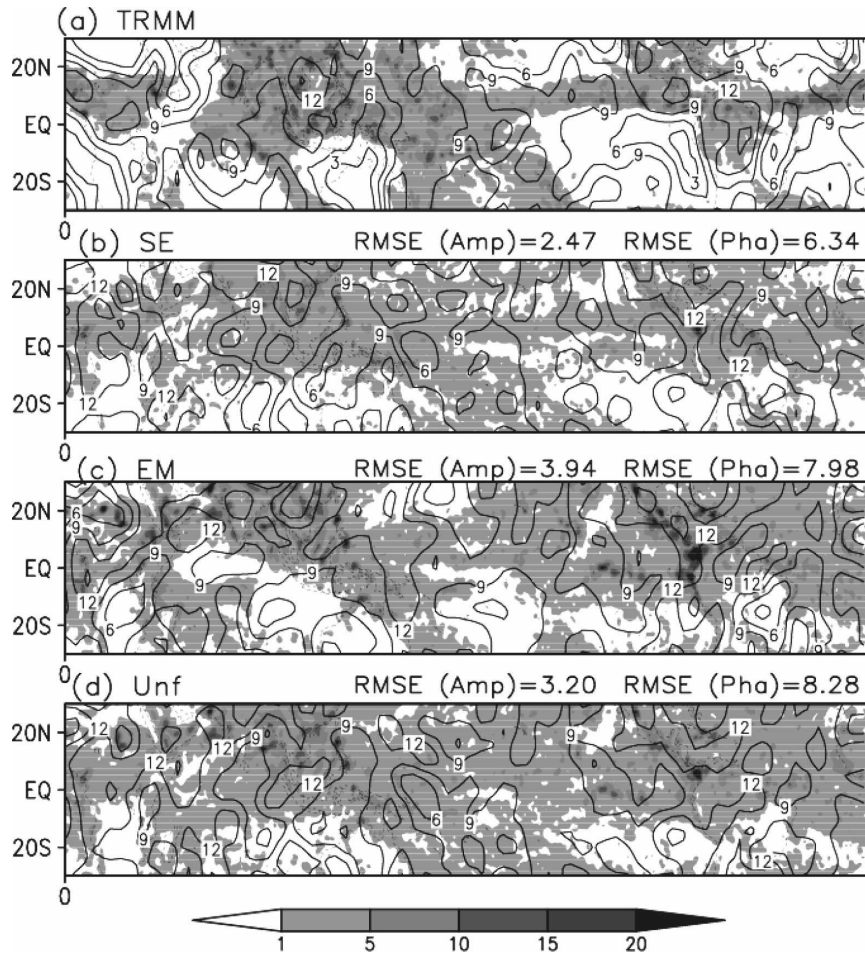


FIG. 4. As in Fig. 3 but for day 5.

the filtered data over the total number of forecast days is the representative diurnal cycle for that period of time. It was found that the diurnal cycle obtained using this method is very close (within 1% of errors) to the  $n$ th harmonic of the  $n$ -daylong time series of data. Hence  $n$  refers to day 1 to day 5.

The TRMM data-based observed estimates of diurnal changes were based on the 3-hourly TRMM 3B42 dataset (Huffman et al. 2001, 2007). The shading illustrates the amplitude of the diurnal change (in  $\text{mm day}^{-1}$ ), which has a rather large spread over most of the tropics for the ensemble mean and for the unified model. These are corrected to more reasonable values from the use of the multimodel superensemble. Here we show the results from the TRMM 3B42 datasets, the multimodel superensemble, the ensemble mean, and from the unified model. The rms errors for the diurnal amplitude over the tropical belt from  $30^{\circ}\text{S}$  to  $30^{\circ}\text{N}$  were 2.34, 4.24, and  $3.12 \text{ mm day}^{-1}$  for the superensemble, ensemble mean, and the unified model, respectively, and for the phase these were 6.39, 8.45, and  $8.34 \text{ h}$ ,

respectively. This shows that one can predict the amplitudes and phase of the diurnal change of precipitation with considerable improvement using the multimodel superensemble compared to using an ensemble mean, which reflects the behavior of the member models. The unified model is somewhat better in performance compared to the ensemble mean.

The geographical distribution of the phase and amplitude of diurnal precipitation for day 5 of the forecasts is shown in Fig. 4. The rms errors for the amplitude and phase are displayed as in the previous figure. The results on day 5 are quite similar to those for day 2 of the forecasts. Here we again find a superior performance for the multimodel superensemble compared to those of the ensemble mean and the unified model.

### c. Diurnal change over tropical oceans and over land areas

The day 2 and day 5 forecasts over the tropical Pacific, Indian, and Atlantic Oceans and over the land areas are shown in Fig. 5. Here we display a full diurnal

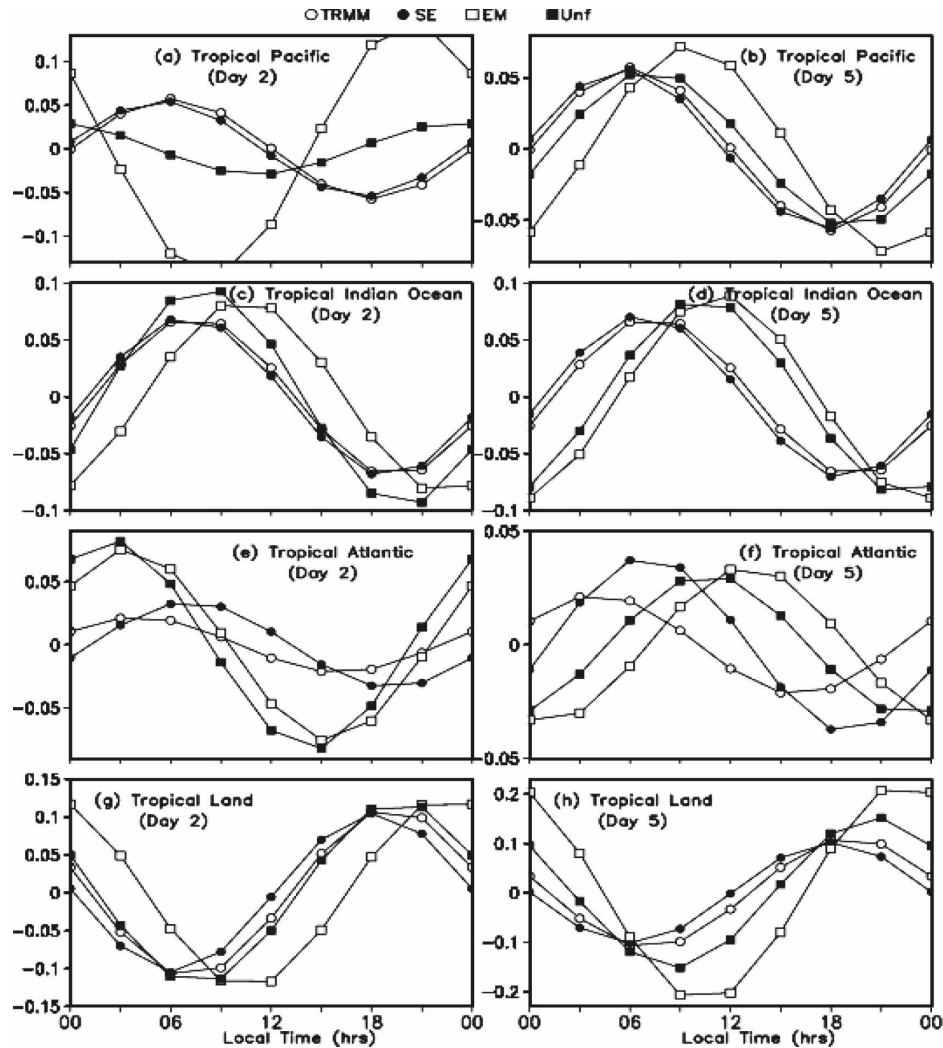


FIG. 5. The full diurnal cycle of precipitation from the TRMM rainfall estimates, from the superensemble, the ensemble mean, and the unified model over the tropical ocean and land areas. The diurnal cycle of (left) day 2 forecasts; (right) day-5 forecasts ( $\text{mm day}^{-1}$ ) over (a), (b) the tropical Pacific; (c), (d) the tropical Indian Ocean; (e), (f) the tropical Atlantic; and (g), (h) tropical land.

cycle of precipitation from the TRMM rainfall estimates and from the superensemble, the ensemble mean, and the unified model. The ensemble mean reflects more closely the behavior of the member models. Day 2 forecasts are illustrated in the left panels and day 5 forecasts are displayed on the right. The TRMM-based phase and amplitude are very closely predicted by the multimodel superensemble through the 24-h cycle in all regions. The phase errors of the ensemble mean are much larger. The superensemble removes the systematic errors in the models and improves the diurnal phase and amplitude forecast. The errors over the Pacific Ocean, the Indian Ocean, and the land areas are clearly the least for the multimodel superensemble for days 2 and 5 of the forecast. The errors over the At-

lantic Ocean seem to be slightly higher, but improvements over the Atlantic are quite significant. The large differences in phase between land (afternoon maximum) and oceans (early morning maximum) is well predicted by the superensemble, which captures the entire diurnal cycle of the precipitation forecast very close to the observed estimates from TRMM. We also note that the errors over the land areas are slightly larger compared to those over oceans. The unified model provided an improvement in the forecasts of the phase of the diurnal change of precipitation for days 2 and 5 forecasts with respect to the ensemble mean over all ocean basins and the land area. It appears from this analysis that a reasonable prediction of the diurnal change through day 5 of the forecast can be achieved

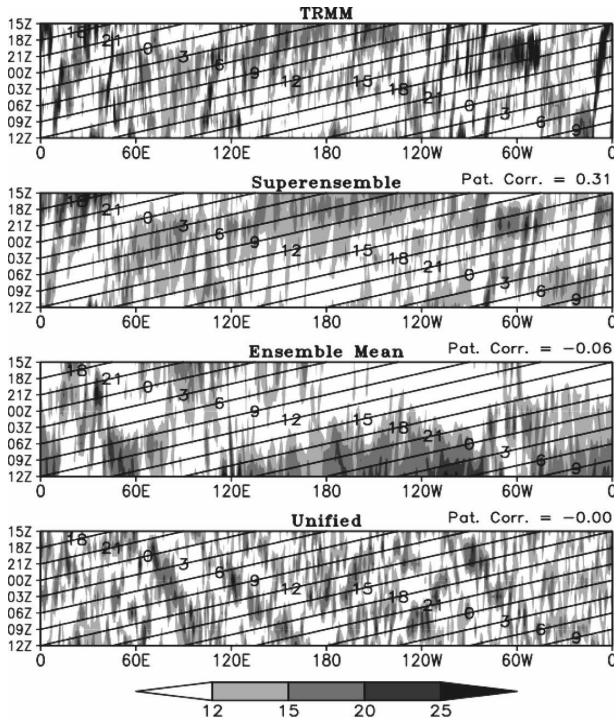


FIG. 6. Time-longitude diagram averaged between  $5^{\circ}\text{S}$  and  $5^{\circ}\text{N}$  illustrating the zonal passage of equatorial rain. Rainfall rates ( $\text{mm day}^{-1}$ ) are shaded, and slanted lines denote lines of equal local time. (top) TRMM estimates and day-5 forecast (upper middle) using the superensemble, (lower middle) ensemble mean, and (bottom) unified model.

from the deployment of the superensemble. The success of the superensemble lies in the persistence of the systematic errors of the member models and the TRMM database that provides the training coefficients. In fact, the superensemble corrects the inherent systematic bias in the member models and provides an improved forecast.

#### d. Diurnal rains following the sun

Using TRMM datasets, Yang and Smith (2006) provided a longitude-time diagram illustrating the zonal passage of equatorial rain (averaged between  $5^{\circ}\text{S}$  and  $5^{\circ}\text{N}$ ). For our experiment we have reconstructed that format in Fig. 6. Here we show the results based on TRMM data and the day-5 forecasts from the superensemble, the ensemble mean, and the unified model. Rainfall rates ( $\text{mm day}^{-1}$ ) are shaded, and the slanted lines from bottom left to top right denote lines of equal local time. This illustration is intended to show how the observed behavior of the diurnal phase of rain follows the sun and how the various versions of the forecasts capture the observed features. The TRMM rainfall estimates show the following features: In the Atlantic be-

tween  $20^{\circ}$  and  $40^{\circ}\text{W}$  longitude moderate diurnal rainfall maxima occur in the early morning hours from 0600 to 0900 local time. Near  $60^{\circ}\text{W}$  we note heavy afternoon showers centered between 1500 and 1800 local time. Most of the equatorial Pacific Ocean carries a moderate diurnal rainfall maxima centered on 0600 local time. It is interesting to note here that the westward passage of equatorial rain follows the sun between roughly  $150^{\circ}\text{W}$  and  $120^{\circ}\text{E}$ . Thereafter the effects of land convection broaden the span of diurnal convection between 0300 and 1800 local time. Some of the heaviest diurnal rains are seen over equatorial Africa near  $30^{\circ}\text{E}$ , the west coast of Africa (heaviest rains before midnight and noon hour). When one looks at the same format of rainfall representation for the unified model and the ensemble mean the results are, in fact, quite out of phase in several regions. The equatorial Pacific Oceans (for these forecasts) show heavy rains between 1500 and 0600 local time. Heavy rains are also predicted between 0900 and 1500 local time near  $50^{\circ}\text{E}$ . These features are not present in the TRMM-based observed rainfall estimates. Most of the features of moderate to heavy rains seen on TRMM are not predicted at the correct local time; in general, the phase errors are  $O(9\text{--}12\text{ h})$ . However, the model errors seem to be very consistent from one forecast to the next, which provided stable statistical weights for the multimodel superensemble. This enabled us to construct a superensemble-based forecast for day 5 that was quite superior compared to the best model and the ensemble mean. The respective spatial correlations for the superensemble, the ensemble mean, and the unified model for the diurnal change of precipitation over the equatorial latitudes were 0.31,  $-0.06$ , and  $-0.003$ .

#### e. Some local regions

The member models exhibit largest errors in predicting the phase and amplitude over the eastern Tibetan Plateau, the eastern foothills of Himalayas, and the Amazon basin (Krishnamurti et al. 2007). Over a distance of the same 500 km a strong phase shift in diurnal rainfall is noted between the eastern Tibetan Plateau and the region of heavy rain over the eastern foothills of the Himalayas. Over the eastern Tibetan Plateau the observed diurnal rainfall maxima are noted around 1800 local time, whereas the local maxima over the eastern foothills are around 0600 (Figure 7 illustrates the predictions of the diurnal phase and amplitude of precipitation over these regions). The forecast based on the superensemble reduces these model errors drastically for the phase and amplitude to values quite close to the observed estimates from the TRMM datasets. The ensemble means reflect the behavior of the indi-

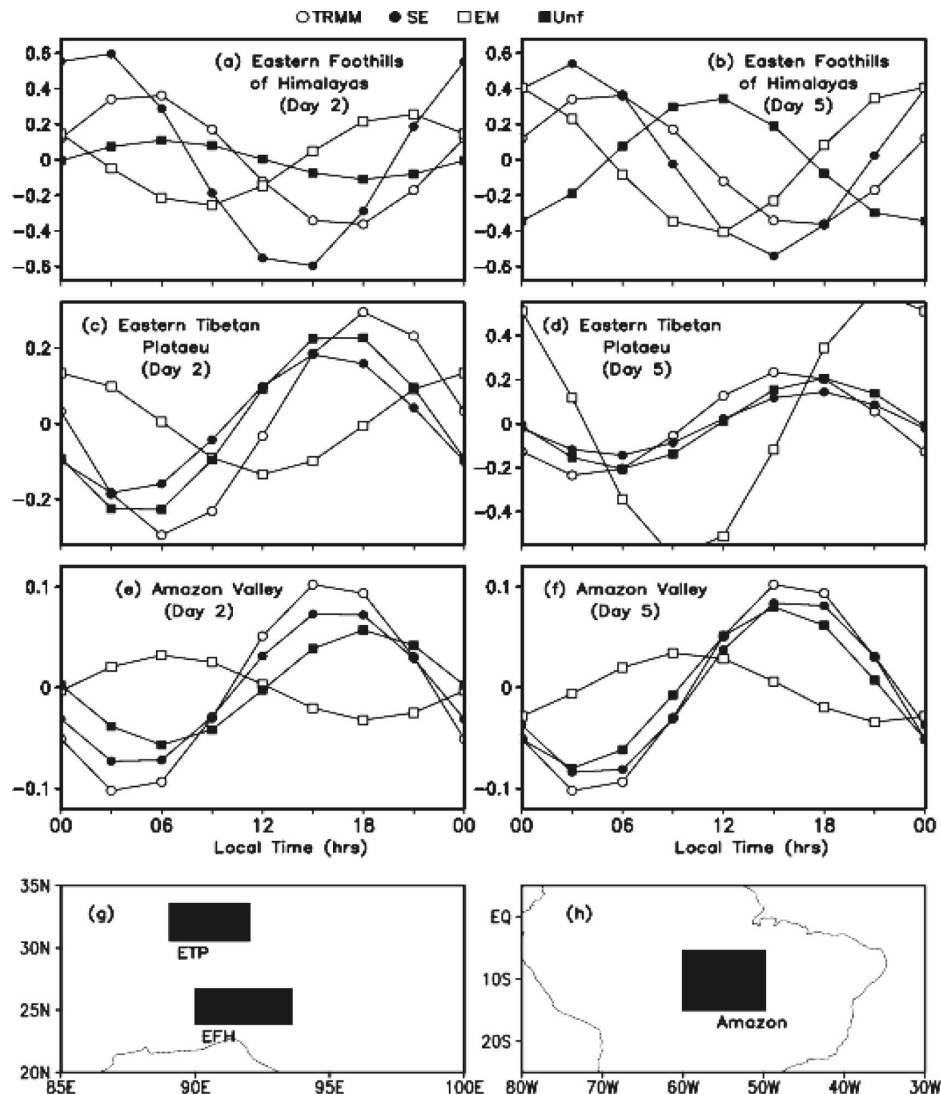


FIG. 7. Diurnal cycle of precipitation from the TRMM rainfall estimates using the superensemble, the ensemble mean, and the unified model over selected domains: diurnal cycle of (left) day-2 forecasts and (right) day-5 forecasts over (a), (b) eastern foothills of the Himalayas; (c), (d) eastern Tibetan Plateau; and (e), (f) the Amazon basin. (g), (h) The domain of interest is highlighted.

vidual member models that have rather large phase errors. Such large phase errors (by as much as 12 h) were also noted for the ensemble mean over the Amazon basin. The systematic errors in these models for days 2 and 5 of the forecasts were very persistent, and it was possible for the superensemble to correct such systematic errors and provide forecasts through day 5 that were very close to the observed estimates from TRMM.

The phase and amplitude of the diurnal rainfall varies a lot over the tropical belt. An early morning rainfall maximum over oceans and a late afternoon rainfall over land area is not the norm for all regions. Large differences over short distances, such as the Tibetan

Plateau and the eastern foothills of the Himalayas, are attributed to a number of factors. The reduction of sensible heating over sloping terrain in the lower troposphere and larger albedo of high clouds over the foothills, compared to what the models have been using, contributes to stabilization in the afternoon hours, the early morning maximum over the region is attributed to the nocturnal destabilization of high clouds from long-wave radiation. The eastern plateau encounters mostly shallower towering cumulus clouds; this exhibits the largest growth from the afternoon surface heating of the plateau. The member models have phase errors as large as 9–12 h over these regions and do not distin-

TABLE 1. Rms errors for the superensemble (SE), ensemble mean (EM), and unified model (Unf) in the (a) amplitude and (b) phase for day-2 and day-5 forecasts using different cloud radiative transfer and cumulus parameterization experiments.

Expt	(a) Amplitude			(b) Phase		
	Day 2					
	SE	EM	Unf	SE	EM	Unf
Cloud radiative transfer	3.48	3.70	3.81	5.98	7.73	7.87
Cumulus parameterization	2.34	4.24	3.12	6.39	8.45	8.34
Expt	Day 5					
	SE	EM	Unf	SE	EM	Unf
	Cloud radiative transfer	3.31	3.84	3.94	5.86	8.23
Cumulus parameterization	2.47	3.94	3.20	6.34	7.98	8.28

guish between the plateau and the foothills. The geographical locations of the local region described above are identified in Figs. 7g and 7h.

#### f. Statistical significance

In this section we address the issue of the significance of the superensemble forecasts over the ensemble forecasts. Here we assume that the rms errors of the member models are normally distributed. The compound hypothesis is (Green and Margerison 1978, p. 130)

$$H_0: \text{RMSE}_{\text{em}} - \text{RMSE}_{\text{se}} = 0$$

$$H_1: \text{RMSE}_{\text{em}} - \text{RMSE}_{\text{se}} \neq 0,$$

where  $H_0$  is the null hypothesis and  $H_1$  is the alternate hypothesis;  $\text{RMSE}_{\text{em}}$  and  $\text{RMSE}_{\text{se}}$  are the population rms errors of the ensemble mean and superensemble. From the sample estimates of the mean and variances, the  $t$  test parameter can be written as

$$t_s = \frac{|\text{RMSE}_{\text{em}} - \text{RMSE}_{\text{se}}|}{s_{\bar{D}}},$$

where  $s_{\bar{D}} = s_D/\sqrt{n}$  and  $s_D$  is the standard deviation of RMSE within the ensemble of  $n$  members. The hypothesis  $H_0$  is rejected with  $(1 - \alpha)$  100% confidence if  $|t_s| > t_{(1-\alpha/2), n-1}$ . That is,  $\text{RMSE}_{\text{em}}$  and  $\text{RMSE}_{\text{se}}$  differ with a significance level more than  $(1 - \alpha)$  100% when the above condition is satisfied. The significance level was calculated by solving the above equation for  $\alpha$  with known values of  $\text{RMSE}_{\text{em}}$ ,  $\text{RMSE}_{\text{se}}$ ,  $s_D$ , and  $n$ . The significance test on the difference in RMSE shows that the improvement of superensemble forecast over the ensemble mean forecast is statistically significant at a level generally  $>99\%$  for all of the days of the forecasts.

### 5. Comparison of results from different cloud radiative-transfer-based and different cumulus-parameterization-based multimodels

The diurnal change is affected by both cloud radiative transfer processes and by the heating of the surface

layer and related convective processes. We have conducted a large number of multimodel forecasts for these two areas of modeling. The first of these dealing with impacts on diurnal changes from diverse cloud radiative transfer were discussed in Krishnamurti et al. (2007). This present study explores the effects on the diurnal change of precipitation from a suite of diverse cumulus parameterization algorithms within multimodels. Here we address the question whether the cloud radiation or the cumulus convection (within multimodels) is contributing much to the phase and amplitude of the diurnal change of rainfall. Table 1 shows the rms errors for day 2 and day 5 of the forecasts (from the two suites of multimodels: those that use different cloud radiative transfer algorithms and those that use different cumulus parameterization schemes). Table 1b shows that the multimodel superensemble does provide the largest improvements for the amplitude of diurnal change forecasts compared to the ensemble mean for both cases. It is important to note that the errors are less when a suite of models carrying different cumulus parameterizations is deployed. The use of diverse cloud radiative transfer processes does reduce these errors to the level of rms = 3.48 mm day<sup>-1</sup> (day 2) and 3.31 mm day<sup>-1</sup> (day 5), but a further reduction to rms = 2.34 mm day<sup>-1</sup> (day 2) and 2.47 mm day<sup>-1</sup> (day 5) was provided with the diverse cumulus parameterization schemes (Table 1a). However, Table 1b shows that the phase of diurnal change forecast from both experiments is comparable. This suggests that, while modeling the diurnal change of precipitation both cloud radiative transfer processes and surface heating processes (that reflect in the behavior of cumulus convection) are important but more care must be taken on parameterizing the cumulus convection.

The robustness of the multimodel superensemble was noted in Krishnamurti and Sanjay (2003); here we found a large impact in forecasts from the use of the multimodels that carry different cumulus parameterization schemes. Each of these member models have sub-

stantial errors for the diurnal cycle; however, the nature of these diurnal errors was noted to be very systematic from one forecast to the next. The superensemble is ideally suited for reducing such systematic errors, which was the reason for the enhanced skills for the diurnal cycle reported in this study.

## 6. Concluding remarks

We have shown that it is possible to improve the prediction of the phase and amplitude of predicted diurnal rain over the entire tropics on a time scale from 1 to 5 days from the construction of the multimodel superensemble. This can be done using a suite of models. Each member model of that suite utilizes a different cumulus parameterization algorithm. This list of cumulus parameterization covers some of the best state-of-the-art algorithms. It was difficult to assess superiority of one cumulus parameterization scheme over another in the context of the diurnal change issue. The reason for that is they all carry rather large systematic errors. Such errors arise not only from the use of single schemes but also from the way multischemes interact with the rest of the model structure. It should be stated that all of the diurnal change in the atmosphere and ocean stems from a single parameter in modeling, that is, the solar zenith angle within the shortwave radiative transfer algorithm. If that were set to a constant in a model the entire diurnal change would disappear. The information from the solar irradiance is passed on to the cumulus parameterization through the surface and boundary-layer physics.

This study is a sequel to a recent study (Krishnamurti et al. 2007) on the same diurnal change issue. In Krishnamurti et al. (2007) we deployed a suite of multimodels that varied from each other in their use of cloud radiative transfer algorithms. Cloud radiation through cloud albedo and related absorption of shortwave radiation and through possible nocturnal longwave destabilization of clouds can affect the diurnal variation of rain. By choosing a number of different cloud radiative transfer algorithms in different member models, all using the same cumulus parameterization scheme, that is, the relaxed Arakawa–Schubert scheme, it was possible to see the same diverse descriptions for the diurnal change of rainfall. These solutions from member models had large systematic errors for the phase as well as the amplitude for the tropical rainfall. The multimodel superensemble provided superior forecasts for the diurnal changes by reducing such model bias errors. The diurnal changes in the suite of models that use diverse cloud radiative schemes are initiated by the varying zenith angle from within each of the radiative transfer algorithms.

We noted about 50% and 25% reductions in the rms errors for the diurnal phase and amplitude, respectively, for tropical precipitation from the superensemble compared to the best model. The corresponding reductions from the suite of cloud radiative transfer multimodels were 15% and 25%, respectively. The cumulus parameterization-based multimodels seem to carry somewhat improved skills for the diurnal change of tropical precipitation. Major improvements are also reflected over the Tibetan Plateau, the eastern foothills of Himalayas, and the Amazon basin where the model errors are essentially large.

*Acknowledgments.* The data used in this study were acquired as part of TRMM. These algorithms were developed by the TRMM science team. The data were processed by the TRMM Science Data and Information System (TSDIS) and the TRMM office; they are archived and distributed by the Goddard Distributed Active Archive Center (GDAAC). TRMM is an international project jointly sponsored by the Japan Aerospace Exploration Agency (JAXA) and the U.S. National Aeronautics and Space Administration (NASA) office of Earth Science. The study was supported by the following grants: NSF ATM-0419618 and ATM-0311858, NASA NAG5-13563 and NNG05GH81G, and NOAA NA16GP1365.

## REFERENCES

- Arakawa, A., and W. H. Schubert, 1974: Interaction of a cumulus cloud ensemble with the large-scale environment, Part I. *J. Atmos. Sci.*, **31**, 674–701.
- Chakraborty, A., and T. N. Krishnamurti, 2008: Improved forecasts of the diurnal cycle in the tropics using multiple global models. Part II: Asian summer monsoon. *J. Climate*, **21**, 4045–4067.
- , —, and C. Gnanaseelan, 2007: Prediction of the diurnal change using a multimodel superensemble. Part II: Clouds. *Mon. Wea. Rev.*, **135**, 4097–4116.
- Emanuel, K. A., 1991: A scheme for representing cumulus convection in large-scale models. *J. Atmos. Sci.*, **48**, 2313–2335.
- , and M. Zivkovic-Rothman, 1999: Development and evaluation of a convection scheme for use in climate models. *J. Atmos. Sci.*, **56**, 1766–1782.
- Green, J. R., and D. Margerison, 1978: *Statistical Treatment of Experimental Data*. 3rd ed. Elsevier Scientific, 382 pp.
- Grell, G. A., 1993: Prognostic evaluation of assumptions used by cumulus parameterizations. *Mon. Wea. Rev.*, **121**, 764–787.
- Huffman, G. J., R. F. Adler, M. Morrissey, D. T. Bolvin, S. Curtis, R. Joyce, B. McGavock, and J. Susskind, 2001: Global precipitation at one-degree daily resolution from multisatellite observations. *J. Hydrometeorol.*, **2**, 36–50.
- , and Coauthors, 2007: The TRMM Multisatellite Precipitation Analysis (TMPA): Quasi-global, multiyear, combined-sensor precipitation estimates at fine scales. *J. Hydrometeorol.*, **8**, 38–55.
- Krishnamurti, T. N., and H. S. Bedi, 1988: Cumulus parameter-

- ization and rainfall rates: Part III. *Mon. Wea. Rev.*, **116**, 583–599.
- , and J. Sanjay, 2003: A new approach to the cumulus parameterization issue. *Tellus*, **55A**, 275–300.
- , Y. Ramanathan, H. L. Pan, R. J. Pasch, and J. Molinari, 1980: Cumulus parameterization and rainfall rates I. *Mon. Wea. Rev.*, **108**, 465–472.
- , C. M. Kishtawal, T. LaRow, D. Bachiochi, Z. Zhang, C. E. Williford, S. Gadgil, and S. Surendran, 1999: Improved weather and seasonal climate forecasts from multimodel superensemble. *Science*, **285**, 1548–1550.
- , —, T. LaRow, D. Bachiochi, Z. Zhang, C. E. Williford, S. Gadgil, and S. Surendran, 2000a: Improving tropical precipitation forecasts from a multianalysis superensemble. *J. Climate*, **13**, 4217–4227.
- , —, D. W. Shin, and C. E. Williford, 2000b: Multimodel superensemble forecasts for weather and seasonal climate. *J. Climate*, **13**, 4196–4216.
- , and Coauthors, 2001: Real-time multianalysis–multimodel superensemble forecasts of precipitation using TRMM and SSM/I products. *Mon. Wea. Rev.*, **129**, 2861–2883.
- , and Coauthors, 2003: Improved skill for the anomaly correlation of geopotential heights at 500 hPa. *Mon. Wea. Rev.*, **131**, 1082–1102.
- , C. Gnanaseelan, and A. Chakraborty, 2007: Prediction of the diurnal change using a multimodel superensemble Part I: Precipitation. *Mon. Wea. Rev.*, **135**, 3613–3632.
- , S. Basu, J. Sanjay, and C. Gnanaseelan, 2008: Evaluation of several different planetary boundary layer schemes within a single model, a unified model and a multimodel superensemble. *Tellus*, **60A**, 42–61.
- Lord, S. J., and A. Arakawa, 1980: Interaction of a cloud ensemble with the large-scale environment. Part II. *J. Atmos. Sci.*, **37**, 2677–2692.
- , W. C. Chao, and A. Arakawa, 1982: Interaction of a cumulus cloud ensemble with the large-scale environment. Part IV: The discrete model. *J. Atmos. Sci.*, **39**, 104–113.
- Moorthi, S., and M. J. Suarez, 1992: Relaxed Arakawa–Schubert: A parameterization of moist convection for general circulation models. *Mon. Wea. Rev.*, **120**, 978–1002.
- Pan, H.-L., and W. S. Wu, 1995: Implementing a mass flux convection parameterization package for the NMC medium-range forecast model. NMC Office Note 409, 40 pp.
- Pleim, J. E., and A. Xiu, 1995: Development and testing of a surface flux and planetary boundary layer model for application in a mesoscale models. *J. Appl. Meteor.*, **34**, 16–32.
- Raymond, D. J., and A. M. Blyth, 1986: A stochastic mixing model for nonprecipitating cumulus clouds. *J. Atmos. Sci.*, **43**, 2708–2718.
- Reynolds, R. W., and T. M. Smith, 1994: Improved global sea surface temperature analyses using optimum interpolation. *J. Climate*, **7**, 929–948.
- Slingo, A., R. Wilderspin, and S. Brentnall, 1987: Simulation of the diurnal cycle of outgoing longwave radiation with an atmospheric GCM. *Mon. Wea. Rev.*, **115**, 1451–1457.
- Wilks, D. S., 1995: *Statistical Methods in the Atmospheric Sciences*. Academic Press, 467 pp.
- Yanai, M., 1963: A preliminary survey of large-scale disturbances over the tropical Pacific region. *Geofis. Int.*, **3**, 73–84.
- Yang, S., and E. A. Smith, 2006: Mechanisms for diurnal variability of global tropical rainfall observed from TRMM. *J. Climate*, **19**, 5190–5226.
- Yun, W. T., L. Stefanova, and T. N. Krishnamurti, 2003: Improvement of multimodel superensemble technique for seasonal forecasts. *J. Climate*, **16**, 3834–3840.
- Zhang, G. J., and N. A. McFarlane, 1995: Sensitivity of climate simulations to the parameterization of cumulus convection in the Canadian Climate Centre general circulation model. *Atmos.–Ocean*, **33**, 407–446.